PAPER

Iterative MMSE Detection with Interference Cancellation for Up-Link HARQ Using Frequency-Domain Filtered SC-FDMA MIMO Multiplexing

Suguru OKUYAMA[†a)], **Tetsuya YAMAMOTO**[†], **Kazuki TAKEDA**[†], ***Student Members***, ***and*** **Fumiyuki ADACHI**[†], ***Fellow***

SUMMARY In this paper, we propose an iterative minimum mean square error detection with interference cancellation (MMSED-IC) for frequency-domain filtered single carrier (SC)-frequency-division multiple-access (FDMA) uplink transmission. The use of a square-root Nyquist transmit filter reduces the peak-to-average power ratio (PAPR) while increases the frequency-diversity gain. However, if carrier-frequency separation among multiple-access users is kept the same as the one used for the case of roll-off factor α=0 (i.e., brick-wall filter), then the adjacent users' spectra will overlap and multi-user interference (MUI) occurs. The proposed MMSED-IC can sufficiently suppress the MUI from adjacent users while achieving the maximum frequency-diversity gain. We apply the proposed MMSED-IC to a packet access using filtered SC-FDMA, multi-input multi-output (MIMO) multiplexing, and hybrid automatic repeat request (HARQ). It is shown by computer simulation that filtered SC-FDMA with $\alpha = 1$ can achieve higher throughput than orthogonal frequency division multiple access (OFDMA).

key words: *SC-FDMA, MMSED, interference cancellation, frequency-domain filter, MIMO, HARQ*

1. Introduction

In the next generation mobile communication systems, broadband packet data services are demanded. Since the broadband wireless channel is composed of many propagation paths with different time delays, the packet error rate (PER) performance degrades due to inter-symbol interference (ISI) arising from the strong frequency-selectivity of the channel [1], [2]. Orthogonal frequency division multiplexing (OFDM) converts the frequency-selective channel into a number of orthogonal frequency-nonselective channels (sub-carriers) and alleviates the ISI problem [3], [4]. However, OFDM has a problem of high peak-to-average power ratio (PAPR) [5]. On the other hand, single-carrier (SC) transmission has low PAPR. The use of minimum mean square error frequency-domain equalization (MMSE-FDE) makes use of the channel frequency-selectivity to improve the PER performance [6]–[8]. SC combined with frequency-division multiple-access (SC-FDMA) [9] has been adopted as the uplink multiple access technique for 3GPP LTE systems [10].

Manuscript received March 29, 2011.

Manuscript revised August 24, 2011.

[†]The authors are with the Department of Electrical and Communication Engineering, Graduate School of Engineering, Tohoku University, Sendai-shi, 980-8579 Japan.

a) E-mail: okuyama@mobile.ecei.tohoku.ac.jp

DOI: 10.1587/transcom.E94.B.3559

To limit the SC signal bandwidth while reducing the PAPR, square-root Nyquist filters can be used as transmit/receive filters [2], [11]. However, in the 3GPP LTE systems, the ideal brick-wall filter (i.e., a filter of roll-off factor equal to 0) is used for band-limiting each user's transmit signal and the different users' transmit signal spectra are located so as not to overlap each other. As the filter roll-off factor α of the transmit filter increases, the PAPR decreases and furthermore, an additional frequency-diversity gain can be obtained by making use of the excess bandwidth introduced by the transmit filter [12]. However, if the carrier-frequency separation among multiple access users is kept the same as in the case of $\alpha = 0$, the adjacent users' transmit signal spectra are overlapped and the throughput performance degrades due to increased multi-user interference (MUI). In this paper, we call the above SC-FDMA as "filtered SC-FDMA."

In our previous work [13], we proposed an iterative MMSE-FDE with MUI cancellation (MMSE-FDE/MUIC) for frequency-domain square-root Nyquist transmit filtered uplink SC-FDMA with antenna diversity. In MMSE-FDE/MUIC, joint single-user MMSE-FDE & spectrum combining and MUI cancellation is performed for each user. However, when higher level data modulation (e.g., 16QAM) is used, a big PER performance gap from the single-user case is observed.

In this paper, we propose an iterative MMSE detection with interference cancellation (MMSED-IC) scheme for frequency-domain filtered SC-FDMA uplink transmission. In this scheme, joint MMSE detection and cancellation of MUI, inter-antenna interference (IAI), and ISI is performed iteratively. The proposed MMSED-IC can sufficiently suppress the MUI from adjacent users while achieving the maximum frequency-diversity gain. The proposed MMSED-IC is applied to a frequency-domain filtered SC-FDMA multi-input multi-output (MIMO) multiplexing system.

The remainder of this paper is organized as follows. The frequency-domain filtered SC-FDMA MIMO multiplexing system is presented in Sect. 2. In Sect. 3, we describe the proposed MMSED-IC. In Sect. 4, we evaluate PAPR, PER, and throughput performances by computer simulation. Sect. 5 concludes this paper.

2. Transmission System Model

The uplink SC-FDMA (N_t,N_r) MIMO multiplexing transmitter/receiver structure is illustrated in Fig. 1. Throughout the paper, fast Fourier transform (FFT) sample-spaced discrete-time signal representation is used. The Chase combining [14] is assumed for packet combining. A total of U users are transmitting their data simultaneously.

At the uth ($u=0,\ldots,U-1$) user's transmitter, an information bit sequence is turbo encoded, interleaved, and then transformed into a sequence of data modulated symbols. The data modulated symbol sequence is divided into M-symbol each and converted to N_t parallel data symbol blocks by a serial/parallel (S/P) converter. Each data symbol block is transformed into the frequency-domain signal of M orthogonal subcarriers. Then, the square-root Nyquist filter of roll-off factor α is applied (the signal spectrum is spread over $(1+\alpha)M$ subcarriers).

The frequency-domain signal after transmit filtering is mapped over $N_c = U \cdot M$ subcarriers. In this paper, we consider the localized mapping illustrated in Fig. 2. The carrier-frequency separation is kept the same as in the case of α=0. The frequency-domain signal after spectrum mapping is transformed back to the time-domain signal by applying an N_c-point inverse FFT (IFFT). Last N_g samples of each block are copied as a cyclic prefix (CP) and inserted into the guard interval (GI) placed at the beginning of each block.

$U \cdot N_t$ signal blocks are transmitted simultaneously from

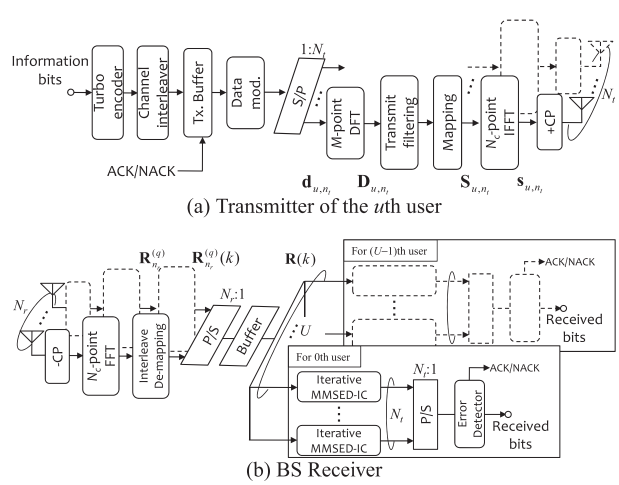

Fig. 1 Transmission system model.

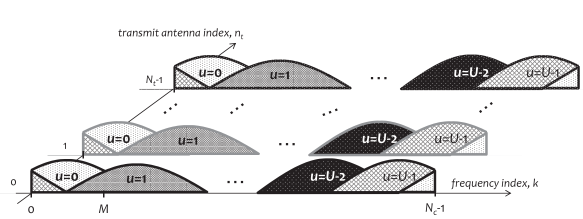

Fig. 2 Spectrum mapping.

N_t transmit antennas. At the BS's n_rth (n_r=0, ..., N_r-1) receive antenna, the received signal block is transformed, after the removal of GI, into the frequency-domain signal by applying an N_c-point FFT. Then, the iterative signal detection is performed $I(\geq 1)$ times for each antenna and each user.

2.1 Transmit Signal Representation

The data symbol block $\mathbf{d}_{u,n_t} = [d_{u,n_t}(0),\ldots,d_{u,n_t}(M-1)]^T$ is first transformed by an M-point discrete Fourier transform (DFT) into frequency-domain signal $\mathbf{D}_{u,n_t} = [D_{u,n_t}(0),\ldots,D_{u,n_t}(M-1)]^T = \mathbf{F}_M \mathbf{d}_{u,n_t}$, to which the transmit filter and localized spectrum mapping are applied. The frequency-domain output $\mathbf{S}_{u,n_t}$=$[S_{u,n_t}(0),\ldots,S_{u,n_t}(N_c-1)]^T$ can be expressed as

$$\mathbf{S}_{u,n_t} = \mathbf{\Phi}_u \mathbf{H}_T \mathbf{D}_{u,n_t}, \tag{1}$$

where $\mathbf{F}_M$ is K-point DFT matrix given as

$$\mathbf{F}_K = \frac{1}{\sqrt{K}} \begin{bmatrix} 1 & 1 & \cdots & 1 \\ 1 & e^{\frac{-j2\pi\cdot1\cdot1}{K}} & \cdots & e^{\frac{-j2\pi\cdot1\cdot(K-1)}{K}} \\ \vdots & \vdots & \ddots & \vdots \\ 1 & e^{\frac{-j2\pi\cdot(K-1)\cdot1}{K}} & \cdots & e^{\frac{-j2\pi\cdot(K-1)\cdot(K-1)}{K}} \end{bmatrix}, \tag{2}$$

and $\mathbf{H}_T$ is the transmit filter matrix of size $2M \times M$, whose (x,y)th (x=0, ..., $2M-1$, y=0, ..., , $M-1$) element $H_T(x,y)$ is given as

$$H_T(x,y) = \begin{cases} f(x-M) & y=(x-M/2)\mathrm{mod}M \\ 0 & otherwise \end{cases}. \tag{3}$$

In this paper, square-root raised cosine Nyquist filter with roll-off factor α is assumed for the transmit filter whose transfer function $\{f(k); k=-M \sim M-1\}$ is given by

$$f(k)= \begin{cases} 1 & 0 \leq |k| \leq \frac{(1-\alpha)}{2}M \\ \cos\left[\frac{\pi}{2\alpha}\left(\frac{|k|}{M}-\frac{1-\alpha}{2}\right)\right] & \frac{(1-\alpha)}{2}M \leq |k| \leq \frac{(1+\alpha)}{2}M \\ 0 & otherwise \end{cases}. \tag{4}$$

$\mathbf{\Phi}_u$ is the localized spectrum mapping matrix of size $N_c \times 2M$, whose (x,y)th ($x=0,\ldots,N_c-1$, $y=0,\ldots,2M-1$) element $\Phi_u(x,y)$ is given as

$$\Phi_u(x,y) = \begin{cases} 1 & x=(y+(u-1/2)M)\mathrm{mod}N_c \\ 0 & otherwise \end{cases}. \tag{5}$$

An N_c-point IFFT is applied to $\mathbf{S}_{u,n_t}$=$[S_{u,n_t}(0),\ldots,S_{u,n_t}(N_c-1)]^T$ to obtain the transmit time-domain signal $\mathbf{s}_{u,n_t} = [s_{u,n_t}(0),\ldots,s_{u,n_t}(N_c-1)]^T$ as

$$\mathbf{s}_{u,n_t} = \sqrt{\frac{2E_{s,u}}{T_s}} \mathbf{F}_{N_c}^H \mathbf{S}_{u,n_t}, \tag{6}$$

where $E_{s,u}$, T_s and $[.]^H$ denote the symbol energy, symbol duration and the Hermitian transpose operation, respectively.

2.2 Received Signal Representation

We assume that the same packet has been transmitted Q times (i.e., the number of retransmission is Q–1). The propagation channel is assumed to be an L-path block fading channel, each path being subjected to independent fading. Let $h^{(q)}_{u,n_t,n_r,l}$ and $\tau_{u,l}$ respectively denote the complex-valued path gain and the delay time of the lth path between the uth user's n_tth transmit antenna and the BS's n_rth receive antenna for the qth ($q=1,\ldots,Q$) packet transmission. The channel impulse response is expressed as

$$h^{(q)}_{u,n_t,n_r}(\tau) = \sum_{l=0}^{L-1} h^{(q)}_{u,n_t,n_r,l}\delta(\tau - \tau_{u,l}), \tag{7}$$

where $\delta(\tau)$ is the delta function. The time delay of each propagation path is assumed to be an integer multiple of the IFFT sampling period. The received signal block on the n_rth received antenna can be expressed using matrix form as

$$\mathbf{r}^{(q)}_{n_r} = \sum_{u=0}^{U-1}\sum_{n_t=0}^{N_t-1} \mathbf{h}^{(q)}_{u,n_t,n_r}\mathbf{s}_{u,n_t} + \mathbf{n}^{(q)}_{n_r}, \tag{8}$$

where $\mathbf{n}^{(q)}_{n_r} = [n^{(q)}_{n_r}(0),\ldots,n^{(q)}_{n_r}(N_c-1)]^T$ is the noise vector with N_c elements being independent zero-mean complex Gaussian variables with variance $2N_0/T_s$ (N_0 is the single-sided power spectrum density of the additive white Gaussian noise (AWGN)) and $\mathbf{h}^{(q)}_{u,n_t,n_r}$ is an $N_c\times N_c$ channel impulse response matrix given as

$$\mathbf{h}^{(q)}_{u,n_t,n_r} = \tag{9}$$
$$\begin{bmatrix} h^{(q)}_{u,n_t,n_r,0} & & & h^{(q)}_{u,n_t,n_r,L-1} & \cdots & h^{(q)}_{u,n_t,n_r,1} \\ \vdots & \ddots & & & \ddots & \vdots \\ & & h^{(q)}_{u,n_t,n_r,0} & \mathbf{0} & & h^{(q)}_{u,n_t,n_r,L-1} \\ h^{(q)}_{u,n_t,n_r,L-1} & & \vdots & \ddots & & \\ & \ddots & & & \ddots & \\ \mathbf{0} & & h^{(q)}_{u,n_t,n_r,L-1} & \cdots & \cdots & h^{(q)}_{u,n_t,n_r,0} \end{bmatrix}.$$

An N_c-point FFT is applied to $\mathbf{r}^{(q)}_{n_r}=[r^{(q)}_{n_r}(0),\ldots,r^{(q)}_{n_r}(N_c-1)]^T$ to transform it into the frequency-domain signal as

$$\begin{aligned}\mathbf{R}^{(q)}_{n_r} &= [R^{(q)}_{n_r}(0),\ldots,R^{(q)}_{n_r}(N_c-1)]^T \\ &= \mathbf{F}_{N_c}\mathbf{r}^{(q)}_{n_r} = \mathbf{F}_{N_c}\sum_{u=0}^{U-1}\sum_{n_t=0}^{N_t-1}\mathbf{h}^{(q)}_{u,n_t,n_r}\mathbf{s}_{u,n_t} + \mathbf{F}_{N_c}\mathbf{n}^{(q)}_{n_r}. \end{aligned}\tag{10}$$

Since $\mathbf{h}^{(q)}_{u,n_t,n_r}$ is a circulant matrix,

$$\begin{aligned}\mathbf{F}_{N_c}\mathbf{h}^{(q)}_{u,n_t,n_r}\mathbf{F}^H_{N_c} &= \mathbf{H}^{(q)}_{u,n_t,n_r} \\ &= diag[H^{(q)}_{u,n_t,n_r}(0),\ldots,H^{(q)}_{u,n_t,n_r}(N_c-1)],\end{aligned}\tag{11}$$

and therefore, Eq. (10) can be rewritten as

$$\mathbf{R}^{(q)}_{n_r} = \sum_{u=0}^{U-1}\sum_{n_t=0}^{N_t-1}\sqrt{\frac{2E_{s,u}}{T_s}}\bar{\mathbf{H}}^{(q)}_{u,n_t,n_r}\mathbf{D}_{u,n_t} + \mathbf{N}^{(q)}_{n_r}, \tag{12}$$

where $\bar{\mathbf{H}}^{(q)}_{u,n_t,n_r}$ is equivalent channel matrix given by $\bar{\mathbf{H}}^{(q)}_{u,n_t,n_r}=\mathbf{H}^{(q)}_{u,n_t,n_r}\mathbf{\Phi}_u\mathbf{H}_T$ and $\mathbf{N}^{(q)}_{n_r} = [N^{(q)}_{n_r}(0),\ldots,N^{(q)}_{n_r}(N_c-1)]^T$ is frequency-domain noise vector at the n_rth receive antenna.

Totally of QN_rN_c signal blocks have been received. They can be expressed using vector $\mathbf{R}$ of size $QN_rN_c\times 1$ as

$$\begin{aligned}\mathbf{R} &= \left[(\mathbf{R}^{(1)}_0)^T\ldots(\mathbf{R}^{(1)}_{N_r-1})^T\ldots(\mathbf{R}^{(Q)}_0)^T\ldots(\mathbf{R}^{(Q)}_{N_r-1})^T\right]^T \\ &= \sum_{u=0}^{U-1}\sum_{n_t=0}^{N_t-1}\sqrt{\frac{2E_{s,u}}{T_s}}\bar{\mathbf{H}}_{u,n_t}\mathbf{D}_{u,n_t} + \mathbf{N},\end{aligned}\tag{13}$$

where $\bar{\mathbf{H}}_{u,n_t} = \left[(\bar{\mathbf{H}}^{(1)}_{u,n_t,0})^T\ldots(\bar{\mathbf{H}}^{(1)}_{u,n_t,N_r-1})^T\ldots(\bar{\mathbf{H}}^{(Q)}_{u,n_t,0})^T\ldots(\bar{\mathbf{H}}^{(Q)}_{u,n_t,N_r-1})^T\right]^T$ is the equivalent channel matrix of size $QN_rN_c\times M$.

3. Iterative MMSED with Interference Cancellation

Adjacent users signal spectra are partially overlapped with the desired user due to transmit filtering. In MIMO multiplexing, N_t transmitted signals share the same bandwidth. The proposed iterative MMSED-IC separates the overlapped spectra and restores the frequency-domain signal transmitted from each user's each antenna by using spectrum combining.

The frequency-domain signal $\hat{\mathbf{D}}^{(i)}_{u,n_t} = [\hat{D}^{(i)}_{u,n_t}(0),\ldots,\hat{D}^{(i)}_{u,n_t}(M–1)]^T$, which corresponds to $\mathbf{D}_{u,n_t}$, after MMSED at the ith ($i=0,\ldots,I-1$) iteration is given as

$$\begin{aligned}\hat{\mathbf{D}}^{(i)}_{u,n_t} &= \mathbf{W}^{(i)}_{u,n_t}\mathbf{R} \\ &= \sqrt{\frac{2E_{s,u}}{T_s}}\mathbf{D}_{u,n_t} + \sqrt{\frac{2E_{s,u}}{T_s}}\left(\mathbf{W}^{(i)}_{u,n_t}\bar{\mathbf{H}}_{u,n_t} - \mathbf{I}\right)\mathbf{D}_{u,n_t} \\ &\quad +\mathbf{W}^{(i)}_{u,n_t}\left(\sum_{u'=0\neq u}^{U-1}\sum_{n'_t=0}^{N_t-1}\sqrt{\frac{2E_{s,u'}}{T_s}}\bar{\mathbf{H}}_{u',n'_t}\mathbf{D}_{u',n'_t}\right) \\ &\quad +\mathbf{W}^{(i)}_{u,n_t}\left(\sqrt{\frac{2E_{s,u}}{T_s}}\sum_{n'_t=0\neq n_t}^{N_t-1}\bar{\mathbf{H}}_{u,n'_t}\mathbf{D}_{u,n'_t}\right)+\mathbf{W}^{(i)}_{u,n_t}\mathbf{N},\end{aligned}\tag{14}$$

where $\mathbf{W}^{(i)}_{u,n_t}$ is the MMSE weight matrix of size $M\times QN_rN_c$.

The receiver structure with MMSED-IC is illustrated in Fig. 3. In this paper, we apply parallel IC (PIC). Frequency-domain MUI, IAI, and ISI cancellation is carried out simultaneously as

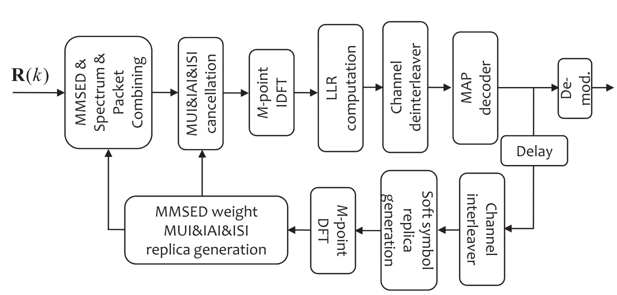

Fig. 3 Receiver structure with iterative MMSED-IC.

$$\check{\mathbf{D}}^{(i)}_{u,n_t} = \hat{\mathbf{D}}^{(i)}_{u,n_t} - \tilde{\mathbf{M}}^{(i)}_{u,n_t} - \tilde{\mathbf{A}}^{(i)}_{u,n_t} - \tilde{\mathbf{I}}^{(i)}_{u,n_t}, \quad (15)$$

where $\tilde{\mathbf{M}}^{(i)}_{u,n_t}$, $\tilde{\mathbf{A}}^{(i)}_{u,n_t}$ and $\tilde{\mathbf{I}}^{(i)}_{u,n_t}$ are respectively the MUI, IAI and ISI replicas which will be shown in 3.1. $\mathbf{W}^{(i)}_{u,n_t}$ in Eq. (14) is the MMSE weight matrix which minimizes the trace of the covariance matrix $E\left[(\mathbf{e}^{(i)}_{u,n_t})(\mathbf{e}^{(i)}_{u,n_t})^H\right]$ of the error vector between $\mathbf{D}^{(i)}_{u,n_t}$ (the transmitted block) and $\check{\mathbf{D}}^{(i)}_{u,n_t}$.

The soft decision symbol $\check{\mathbf{d}}^{(i)}_{u,n_t}=[\check{d}^{(i)}_{u,n_t}(0),\ldots,\check{d}^{(i)}_{u,n_t}(M-1)]^T$ is obtained by applying an M-point IDFT to $\check{\mathbf{D}}^{(i)}_{u,n_t} = [\check{D}^{(i)}_{u,n_t}(0),\ldots,\check{D}^{(i)}_{u,n_t}(M-1)]^T$ as

$$\check{\mathbf{d}}^{(i)}_{u,n_t} = \mathbf{F}^H_M \check{\mathbf{D}}^{(i)}_{u,n_t}. \quad (16)$$

3.1 Generation of $\tilde{\mathbf{M}}^{(i)}_{u,n_t}$, $\tilde{\mathbf{A}}^{(i)}_{u,n_t}$, and $\tilde{\mathbf{I}}^{(i)}_{u,n_t}$

The soft symbol replica $\{\tilde{d}^{(i)}_{u,n_t}(m)\}$ is given as [15]

$$\tilde{d}^{(i-1)}_{u,n_t}(m) = \begin{cases} \frac{1}{\sqrt{2}}\tanh\left(\frac{\lambda^{(i-1)}_{0,u,n_t}(m)}{2}\right) + j\frac{1}{\sqrt{2}}\tanh\left(\frac{\lambda^{(i-1)}_{1,u,n_t}(m)}{2}\right) \text{forQPSK} \\ \frac{1}{\sqrt{10}}\tanh\left(\frac{\lambda^{(i-1)}_{0,u,n_t}(m)}{2}\right)\left\{2+\tanh\left(\frac{\lambda^{(i-1)}_{1,u,n_t}(m)}{2}\right)\right\} \\ +j\frac{1}{\sqrt{10}}\tanh\left(\frac{\lambda^{(i-1)}_{2,u,n_t}(m)}{2}\right)\left\{2+\tanh\left(\frac{\lambda^{(i-1)}_{3,u,n_t}(m)}{2}\right)\right\} \text{for16QAM} \end{cases}, \quad (17)$$

where $\lambda^{(i-1)}_{x,u,n_t}(m)$ is the log-likelihood ratio (LLR) of the xth (x=0, …, $N-1$) bit in the mth symbol in a block (N is the number of bits per symbol and m=0, …, $M-1$). $\lambda^{(i-1)}_{x,u,n_t}(m)$ is given as

$$\begin{aligned} \lambda^{(i-1)}_{x,u,n_t}(m) &= \ln\left(\frac{p^{(i-1)}_{u,n_t}(b_{m,x}=1)}{p^{(i-1)}_{u,n_t}(b_{m,x}=0)}\right) \\ &\approx \frac{\left|\check{d}^{(i-1)}_{u,n_t}(m) - \sqrt{\frac{2E_{s,u}}{T_s}}d^{\min}_{b_{m,x}=0}\right|^2}{2\left(\hat{\sigma}^{(i-1)}_{u,n_t}\right)^2} \\ &\quad - \frac{\left|\check{d}^{(i-1)}_{u,n_t}(m) - \sqrt{\frac{2E_{s,u}}{T_s}}d^{\min}_{b_{m,x}=1}\right|^2}{2\left(\hat{\sigma}^{(i-1)}_{u,n_t}\right)^2}, \end{aligned} \quad (18)$$

where $p^{(i-1)}_{u,n_t}(b_{m,x}=0)$ and $p^{(i-1)}_{u,n_t}(b_{m,x}=1)$ are the *a posteriori* probabilities of the transmitted bit $b_{m,x}$ being $b_{m,x}=0$ and $b_{m,x}=1$, respectively, at the $(i-1)$th iteration stage, $d^{\min}_{b_{m,x}=0}$ (or $d^{\min}_{b_{m,x}=1}$) is the symbol which has the shortest Euclidean distance from $\check{d}^{(i-1)}_{u,n_t}(m)$ and whose xth bit is 0 (or 1) and $2\left(\hat{\sigma}^{(i-1)}_{u,n_t}\right)^2$ is the sum of the variances of the MUI, IAI, ISI, and noise.

The soft decision symbol replica block $\tilde{\mathbf{d}}^{(i-1)}_{u,n_t} = [\tilde{d}^{(i-1)}_{u,n_t}(0),\ldots,\tilde{d}^{(i-1)}_{u,n_t}(M-1)]^T$ is transformed into the frequency domain signal $\tilde{\mathbf{D}}^{(i-1)}_{u,n_t}=[\tilde{D}^{(i-1)}_{u,n_t}(0),\ldots,\tilde{D}^{(i-1)}_{u,n_t}(M-1)]^T$ by applying an M-point DFT as

$$\tilde{\mathbf{D}}^{(i-1)}_{u,n_t} = \mathbf{F}_M \tilde{\mathbf{d}}^{(i-1)}_{u,n_t}, \quad (19)$$

where $\tilde{d}^{(-1)}_{u,n_t}(m) = 0$. The frequency-domain MUI replica $\tilde{\mathbf{M}}^{(i)}_{u,n_t} = [\tilde{M}^{(i)}_{u,n_t}(0),\ldots,\tilde{M}^{(i)}_{u,n_t}(M-1)]^T$, IAI replica $\tilde{\mathbf{A}}^{(i)}_{u,n_t} = [\tilde{A}^{(i)}_{u,n_t}(0),\ldots,\tilde{A}^{(i)}_{u,n_t}(M-1)]^T$ and residual ISI replica $\tilde{\mathbf{I}}^{(i)}_{u,n_t} = [\tilde{I}^{(i)}_{u,n_t}(0),\ldots,\tilde{I}^{(i)}_{u,n_t}(M-1)]^T$ are generated as

$$\tilde{\mathbf{M}}^{(i)}_{u,n_t} = \mathbf{W}^{(i)}_{u,n_t}\left(\sum_{u'=0\neq u}^{U-1}\sum_{n'_t=0}^{N_t-1}\sqrt{\frac{2E_{s,u'}}{T_s}}\bar{\mathbf{H}}_{u',n'_t}\tilde{\mathbf{D}}^{(i-1)}_{u',n'_t}\right), \quad (20)$$

$$\tilde{\mathbf{A}}^{(i)}_{u,n_t} = \sqrt{\frac{2E_{s,u}}{T_s}}\mathbf{W}^{(i)}_{u,n_t}\left(\sum_{n'_t=0\neq n_t}^{N_t-1}\bar{\mathbf{H}}_{u,n'_t}\tilde{\mathbf{D}}^{(i-1)}_{u,n'_t}\right), \quad (21)$$

$$\tilde{\mathbf{I}}^{(i)}_{u,n_t} = \sqrt{\frac{2E_{s,u}}{T_s}}\left(\mathbf{W}^{(i)}_{u,n_t}\bar{\mathbf{H}}_{u,n_t} - \mathbf{I}\right)\tilde{\mathbf{D}}^{(i-1)}_{u,n_t}. \quad (22)$$

Simultaneous cancellation of MUI, IAI, and residual ISI is carried out according to Eq. (15).

3.2 Derivation of $\mathbf{W}^{(i)}_{u,n_t}$

The error vector $\mathbf{e}^{(i)}_{u,n_t}$ between the frequency-domain signal after interference cancellation $\check{\mathbf{D}}^{(i)}_{u,n_t}$ and the transmit frequency-domain signal $\mathbf{D}_{u,n_t}$ is defined as

$$\begin{aligned} \mathbf{e}^{(i)}_{u,n_t} &= [e^{(i)}_{u,n_t}(0),\ldots,e^{(i)}_{u,n_t}(M-1)]^T \\ &= \check{\mathbf{D}}^{(i)}_{u,n_t} - \sqrt{\frac{2E_{s,u}}{T_s}}\mathbf{D}_{u,n_t} \\ &= \sqrt{\frac{2E_{s,u}}{T_s}}\left(\mathbf{W}^{(i)}_{u,n_t}\bar{\mathbf{H}}_{u,n_t} - \mathbf{I}\right)\left(\mathbf{D}_{u,n_t} - \tilde{\mathbf{D}}^{(i-1)}_{u,n_t}\right) \\ &\quad + \mathbf{W}^{(i)}_{u,n_t}\left(\sum_{u'=0\neq u}^{U-1}\sum_{n'_t=0}^{N_t-1}\sqrt{\frac{2E_{s,u'}}{T_s}}\bar{\mathbf{H}}_{u',n'_t}\left(\mathbf{D}_{u',n'_t} - \tilde{\mathbf{D}}^{(i-1)}_{u',n'_t}\right)\right) \\ &\quad + \mathbf{W}^{(i)}_{u,n_t}\left(\sqrt{\frac{2E_{s,u}}{T_s}}\sum_{n'_t=0\neq n_t}^{N_t-1}\bar{\mathbf{H}}_{u,n'_t}\left(\mathbf{D}_{u,n'_t} - \tilde{\mathbf{D}}^{(i-1)}_{u,n'_t}\right)\right) \\ &\quad + \mathbf{W}^{(i)}_{u,n_t}\mathbf{N}. \end{aligned} \quad (23)$$

MMSE weight is the one which minimizes the trace of the covariance matrix of the error vector as

$$\begin{aligned} \mathbf{W}^{(i)}_{u,n_t} &= \arg\min trE\left[\mathbf{e}^{(i)}_{u,n_t}\left(\mathbf{e}^{(i)}_{u,n_t}\right)^H\right] \\ &= \arg\min trE\left[\left(\mathbf{D}_{u,n_t} - \tilde{\mathbf{D}}^{(i-1)}_{u,n_t}\right)\left(\mathbf{D}_{u,n_t} - \tilde{\mathbf{D}}^{(i-1)}_{u,n_t}\right)^H\right]. \end{aligned} \quad (24)$$

By solving $\partial trE\left[\mathbf{e}^{(i)}_{u,n_t}\left(\mathbf{e}^{(i)}_{u,n_t}\right)^H\right]/\partial\mathbf{W}^{(i)}_{u,n_t} = 0$, the MMSE weight at the ith stage is given by

$$\begin{aligned} \mathbf{W}^{(i)}_{u,n_t} &= E_{s,u}\rho^{(i-1)}_{u,n_t}\left(\bar{\mathbf{H}}_{u,n_t}\right)^H \\ &\quad \times\left[\sum_{u'=0}^{U-1}E_{s,u'}\sum_{n'_t=0}^{N_t-1}\rho^{(i-1)}_{u',n'_t}\bar{\mathbf{H}}_{u',n'_t}\left(\bar{\mathbf{H}}_{u',n'_t}\right)^H + N_0\mathbf{I}\right]^{-1}, \end{aligned} \quad (25)$$

where $\rho^{(i)}_{u,n_t}$ is given as [15]

$$\rho^{(i)}_{u,n_t} = E\left[\left|D_{u,n_t}(k) - \tilde{D}^{(i)}_{u,n_t}(k)\right|^2\right]$$

$$\approx \frac{1}{M}\sum_{m=0}^{M-1}\left(E[|d_{u,n_t}(m)|^2] - |\tilde{d}^{(i)}_{u,n_t}(m)|^2\right). \quad (26)$$

In the above equation, $E[|d_{u,n_t}(m)|^2]$ is the expectation of the transmitted mth symbol using the *a posteriori* probability of the transmitted symbols for the given received signal $\mathbf{R}$ and is given by [15]

$$E[|d_u(n)|^2] = \begin{cases} 1 & \text{for QPSK} \\ \frac{4}{10}\tanh\left(\frac{\lambda^{(i-1)}_{1,u,n_t}(m)}{2}\right)+\frac{4}{10}\tanh\left(\frac{\lambda^{(i-1)}_{3,u,n_t}(m)}{2}\right)+1 & \text{for 16QAM} \end{cases}. \quad (27)$$

Since $\bar{\mathbf{H}}_{u,n_t}$ in Eq. (25) includes the transfer function of the transmit filter, the MMSE weight also takes the role of a receive filter matched to the transmit filter. $\bar{\mathbf{H}}_{u',n'_t}$ is the equivalent channel matrix of size $QN_rN_c \times M$, and therefore, the matrix inversion in Eq. (25) requires a computational complexity of $\mathrm{O}((QN_rN_c)^3)$. In the next subsection, we will propose a reduced complexity MMSE weight computation.

3.3 Reduced Complexity MMSE Weight Computation

The minimization of the trace $trE\left[\mathbf{e}^{(i)}_{u,n_t}(\mathbf{e}^{(i)}_{u,n_t})^H\right]$ is equivalent to the minimization of the squared error $\left|e^{(i)}_{u,n_t}(k)\right|$ for $k = 0 \sim M-1$ since $trE\left[\mathbf{e}^{(i)}_{u,n_t}(\mathbf{e}^{(i)}_{u,n_t})^H\right] = \sum_{k=0}^{M-1}|e^{(i)}_{u,n_t}(k)|^2$.

By interchanging the elements $R^{(q)}_{n_r}(k)$, $\mathbf{R}^{(q)}_{n_r}$ can be transformed into a block-diagonal matrix as

$$\begin{aligned}\mathbf{R'}^{(q)}_{n_r} &= \left[(\mathbf{R}^{(q)}_{n_r}(0))^T \ldots (\mathbf{R}^{(q)}_{n_r}(M-1))^T\right]^T \\ &= \begin{bmatrix} \bar{\mathbf{H}}^{(q)}_{n_r}(0) & & & \mathbf{0} \\ & \bar{\mathbf{H}}^{(q)}_{n_r}(1) & & \\ & & \ddots & \\ \mathbf{0} & & & \bar{\mathbf{H}}^{(q)}_{n_r}(M-1)\end{bmatrix}\begin{bmatrix}\mathbf{D}(0) \\ \mathbf{D}(1) \\ \vdots \\ \mathbf{D}(M-1)\end{bmatrix} \\ &\quad + \mathbf{N'}^{(q)}_{n_r},\end{aligned} \quad (28)$$

where $\mathbf{R}^{(q)}_{n_r}(k)$ is the received signal vector of size $U\times 1$ after spectrum de-mapping, $\bar{\mathbf{H}}^{(q)}_{n_r}(k)$ is the equivalent channel matrix of size $U \times UN_t$, given as

$$\mathbf{R}^{(q)}_{n_r}(k) = \mathbf{G}(k)\mathbf{R}^{(q)}_{n_r} \quad (29)$$
$$= \left[R^{(q)}_{n_r}(k), \ldots, R^{(q)}_{n_r}(k+xM), \ldots, R^{(q)}_{n_r}(k+(U-1)M)\right]^T,$$
$$\bar{\mathbf{H}}^{(q)}_{n_r}(k) = \quad (30)$$
$$\left[\bar{\mathbf{H}}^{(q)}_{0,0,n_r}(k) \ldots \bar{\mathbf{H}}^{(q)}_{0,N_t-1,n_r}(k) \ldots \bar{\mathbf{H}}^{(q)}_{U-1,0,n_r}(k) \ldots \bar{\mathbf{H}}^{(q)}_{U-1,N_t-1,n_r}(k)\right],$$
$$\mathbf{D}(k) = \quad (31)$$
$$[D_{0,0}(k), \ldots, D_{0,N_t-1}(k), \ldots, D_{U-1,0}(k), \ldots, D_{U-1,N_t-1}(k)]^T,$$

where $\mathbf{G}(k)$ is the spectrum de-mapping matrix of size $U \times N_c$, whose (x, y)th (x=0, ..., U–1, y=0, ..., N_c–1) element $G_{xy}(k)$ being given as

$$G_{xy}(k) = \begin{cases} 1 & y-k = xM \\ 0 & otherwise \end{cases}. \quad (32)$$

Since the channel matrix in Eq. (28) is block diagonal, Eq. (28) can be rewritten as

$$\begin{aligned}\mathbf{R}^{(q)}_{n_r}(k) &= \mathbf{G}(k)\mathbf{R}^{(q)}_{n_r} \\ &= \bar{\mathbf{H}}^{(q)}_{n_r}(k)\mathbf{D}(k) + \mathbf{N}^{(q)}_{n_r}(k) \\ &= \sum_{u=0}^{U-1}\sum_{n_t=0}^{N_t-1}\sqrt{\frac{2E_{s,u}}{T_s}}\bar{\mathbf{H}}^{(q)}_{u,n_t,n_r}(k)D_{u,n_t}(k) + \mathbf{N}^{(q)}_{n_r}(k),\end{aligned} \quad (33)$$

where $\bar{\mathbf{H}}^{(q)}_{u,n_t,n_r}(k)$ is the equivalent channel matrix of size $U\times 1$, given as

$$\bar{\mathbf{H}}^{(q)}_{u,n_t,n_r}(k) = \mathbf{G}(k)\bar{\mathbf{H}}^{(q)}_{u,n_t,n_r}\mathbf{C}(k), \quad (34)$$

with $\mathbf{C}(k)$ being an $U \times 1$ vector whose kth element is 1 and the others are 0.

It can be shown that the kth frequency component $D_{u,n_t}(k)$ transmitted from the n_tth antenna of the uth user appears only in $\mathbf{R}^{(q)}_{n_r}(k)$. Thus, it is sufficient to consider $\mathbf{R}^{(q)}_{n_r}(k)$ for the estimation of $D_{u,n_t}(k)$. All the received signal vector $\mathbf{R}(k)$ is written as

$$\begin{aligned}&\mathbf{R}(k) \\ &= \left[\left(\mathbf{R}^{(1)}_0(k)\right)^T \ldots \left(\mathbf{R}^{(1)}_{N_r-1}(k)\right)^T \ldots \left(\mathbf{R}^{(Q)}_0(k)\right)^T \ldots \left(\mathbf{R}^{(Q)}_{N_r-1}(k)\right)^T\right]^T \\ &= \sum_{u=0}^{U-1}\sum_{n_t=0}^{N_t-1}\sqrt{\frac{2E_{s,u}}{T_s}}\bar{\mathbf{H}}_{u,n_t}(k)D_{u,n_t}(k) + \mathbf{N}(k),\end{aligned} \quad (35)$$

where $\bar{\mathbf{H}}_{u,n_t}(k) = \left[\left(\bar{\mathbf{H}}^{(1)}_{u,n_t,0}(k)\right)^T \ldots \left(\bar{\mathbf{H}}^{(1)}_{u,n_t,N_r-1}(k)\right)^T \ldots \left(\bar{\mathbf{H}}^{(Q)}_{u,n_t,0}(k)\right)^T \ldots \left(\bar{\mathbf{H}}^{(Q)}_{u,n_t,N_r-1}(k)\right)^T\right]^T$ is a $QN_rU \times 1$ channel matrix for the uth user's n_r-th transmit antenna.

MMSE estimation is performed as

$$\begin{aligned}\hat{D}^{(i)}_{u,n_t}(k) &= \mathbf{W}^{(i)}_{u,n_t}(k)\mathbf{R}(k) \\ &= \sqrt{\frac{2E_{s,u}}{T_s}}D_{u,n_t}(k) \\ &\quad + \sqrt{\frac{2E_{s,u}}{T_s}}\left(\mathbf{W}^{(i)}_{u,n_t}(k)\bar{\mathbf{H}}_{u,n_t}(k) - 1\right)D_{u,n_t}(k) \\ &\quad + \mathbf{W}^{(i)}_{u,n_t}(k)\left(\sum_{u'=0\neq u}^{U-1}\sum_{n'_t=0}^{N_t-1}\sqrt{\frac{2E_{s,u'}}{T_s}}\bar{\mathbf{H}}_{u',n'_t}(k)D_{u',n'_t}(k)\right) \\ &\quad + \mathbf{W}^{(i)}_{u,n_t}(k)\left(\sqrt{\frac{2E_{s,u}}{T_s}}\sum_{n'_t=0\neq n_t}^{N_t-1}\bar{\mathbf{H}}_{u,n'_t}(k)D_{u,n'_t}(k)\right) \\ &\quad + \mathbf{W}^{(i)}_{u,n_t}(k)\mathbf{N}(k),\end{aligned} \quad (36)$$

where $\mathbf{W}^{(i)}_{u,n_t}(k)$ is the MMSED weight matrix of size $1 \times QN_rU$ which minimizes the MSE $E\left[|e^{(i)}_{u,n_t}(k)|^2\right]$ between $D_{u,n_t}(k)$ (the kth frequency component of the transmitted symbol block) and $\breve{D}^{(i)}_{u,n_t}(k)$ (the kth frequency component of the soft decision symbol block after interference cancellation), given as

$$\mathbf{W}^{(i)}_{u,n_t}(k) = E_{s,u}\rho^{(i-1)}_{u,n_t}\left(\bar{\mathbf{H}}_{u,n_t}(k)\right)^H$$

$$\times\left[\sum_{u'=0}^{U-1}E_{s,u'}\sum_{n_t'=0}^{N_t-1}\rho_{u',n_t'}^{(i-1)}\bar{\mathbf{H}}_{u',n_t'}(k)\left(\bar{\mathbf{H}}_{u',n_t'}(k)\right)^H+N_0\mathbf{I}\right]^{-1}. \quad (37)$$

It can be understood from Eq. (37) that the inverse matrix computation has an order of $O((QN_rU)^3)$.

The kth frequency-domain MUI replica $\tilde{M}_{u,n_t}^{(i)}(k)$, IAI replica $\tilde{A}_{u,n_t}^{(i)}(k)$ and residual ISI replica $\tilde{I}_{u,n_t}^{(i)}(k)$ are generated as

$$\tilde{M}_{u,n_t}^{(i)}(k)=\mathbf{W}_{u,n_t}^{(i)}(k)\left(\sum_{u'=0\neq u}^{U-1}\sum_{n_t'=0}^{N_t-1}\sqrt{\frac{2E_{s,u'}}{T_s}}\bar{\mathbf{H}}_{u',n_t'}(k)\tilde{D}_{u',n_t'}^{(i-1)}(k)\right), \quad (38)$$

$$\tilde{A}_{u,n_t}^{(i)}(k)=\sqrt{\frac{2E_{s,u}}{T_s}}\mathbf{W}_{u,n_t}^{(i)}(k)\left(\sum_{n_t'=0\neq n_t}^{N_t-1}\bar{\mathbf{H}}_{u,n_t'}(k)\tilde{D}_{u,n_t'}^{(i-1)}(k)\right), \quad (39)$$

$$\tilde{I}_{u,n_t}^{(i)}(k)=\sqrt{\frac{2E_{s,u}}{T_s}}\left(\mathbf{W}_{u,n_t}^{(i)}(k)\bar{\mathbf{H}}_{u,n_t}(k)-1\right)\tilde{D}_{u,n_t}^{(i-1)}(k). \quad (40)$$

4. Computer Simulation

The simulation condition is summarized in Table 1. A packet access using filtered SC-FDMA, (N_t, N_r) MIMO multiplexing, and HARQ is considered. Chase combining [14] is assumed for packet combining. The number of symbols per block is M=64. QPSK and 16QAM data modulations are considered. The information bit sequence length is 1530 bits. A turbo encoder with two (13,15) RSC encoders and a turbo decoder with Log-MAP algorithm are used. The turbo encoder produces the systematic bit sequence (the information bit sequence) and two parity bit sequences. Therefore, an original coding rate is 1/3. To increase the coding rate to 1/2 and 3/4, the two parity bit sequences are punctured.

Table 1 Simulation condition.

Channel coding	No. of information bits	1530 (=1packet)
	Encoder	(13,15)RSC
	Coding rate	$R = 1/2, 3/4$
	Channel interleaver	Block
	Packet combining	Chase combining
	Decoder	Log-MAP
Numbers of Tx and Rx antennas		$N_t = N_r = 4$
Transmitter	Data modulation	QPSK, 16QAM
	No. of symbols per block	$M = 64$
	FFT/IFFT size	$N_c = 256$
	No. of users	$U = 4\ (= N_c/M)$
	CP length	$N_g = 32$ samples
Transmit filter	Transfer function	Square-root raised cosine
	Roll-off factor	$\alpha = 0 \sim 1$
Channel	Fading type	Frequency-selective block Rayleigh
	Power delay profile	L = 16-path exponential power delay profile
	Decay factor	$\beta = 0, 3$ dB
	Time delay	$\tau_{u,l} = l, l = 0 \sim L-1$
Receiver	Signal detection	MMSED-IC
	No. of iterations, I	20 times at the most
	Channel estimation	Ideal

The propagation channel for each pair of transmit and receive antennas is assumed to be an L=16-path frequency-selective block Rayleigh fading channel having the exponential power delay profile with the decay factor β. No correlation among the propagation paths is assumed. We perform I times iterations which is big enough to obtain a sufficient PER improvement but 20 times at the most. The transmit timing is asynchronous among different users, but it is assumed to be kept within the GI. Ideal channel estimation and ideal slow transmit power control ($E_{s,u}$=E_s for all user) are also assumed.

4.1 PAPR

PAPR is defined as [9]

$$\text{PAPR} = \frac{\max\left\{|s_{u,n_t}(t)|^2\right\}_{t=0\sim N_c-1}}{E\left[|s_{u,n_t}(t)|^2\right]}. \quad (41)$$

The PAPR level in dB at the complementary cumulative distribution function (CCDF)=10^{-3} is shown in Table 2 for various values of the roll-off factor α [13]. As α increases, the $\text{PAPR}_{0.1\%}$ level decreases, but it becomes almost the same beyond $\alpha = 0.5$.

4.2 Achievable PER Performance Using Proposed Scheme

No packet retransmission & combining is considered (i.e., Q=1). The PER performance is plotted in Fig. 4 as a function of the average received symbol energy-to-AWGN noise power spectrum density ratio E_s/N_0 when the roll-off factor $\alpha = 0$ and 1. The dacay factor $\beta = 0$ (corresponding to the uniform power delay profile) is assumed. For comparison, the performance without IC (note that 20 decoding iterations are performed in the turbo decoder) is also plotted.

The proposed MMSED-IC improves the PER performance compared with w/o IC since it can suppress the interference (MUI&IAI&ISI) while achieving a higher frequency-diversity and coding gains. In the case of no IC, the PER performance when α=1 degrades compared to when $\alpha = 0$ since larger MUI is present. However, by the use of MMSED-IC, α=1 provides better PER performance. This is because the additional frequency-diversity gain can be obtained by exploiting the excess bandwidth introduced by the transmit filtering.

4.3 Throughput Performance

One packet consists of 1530 information bits. Each user is allocated $(1 + \alpha)M$ subcarriers. However, by allowing the spectrum overlapping between adjacent users, the same

Table 2 PAPR level at CCDF= 10^{-3}.

		SC-FDMA					OFDMA
α		0	0.25	0.5	0.75	1	
PAPR(dB)	QPSK	7.10	5.06	3.37	3.37	3.59	9.98
	16QAM	7.90	6.76	6.46	6.86	7.20	9.77

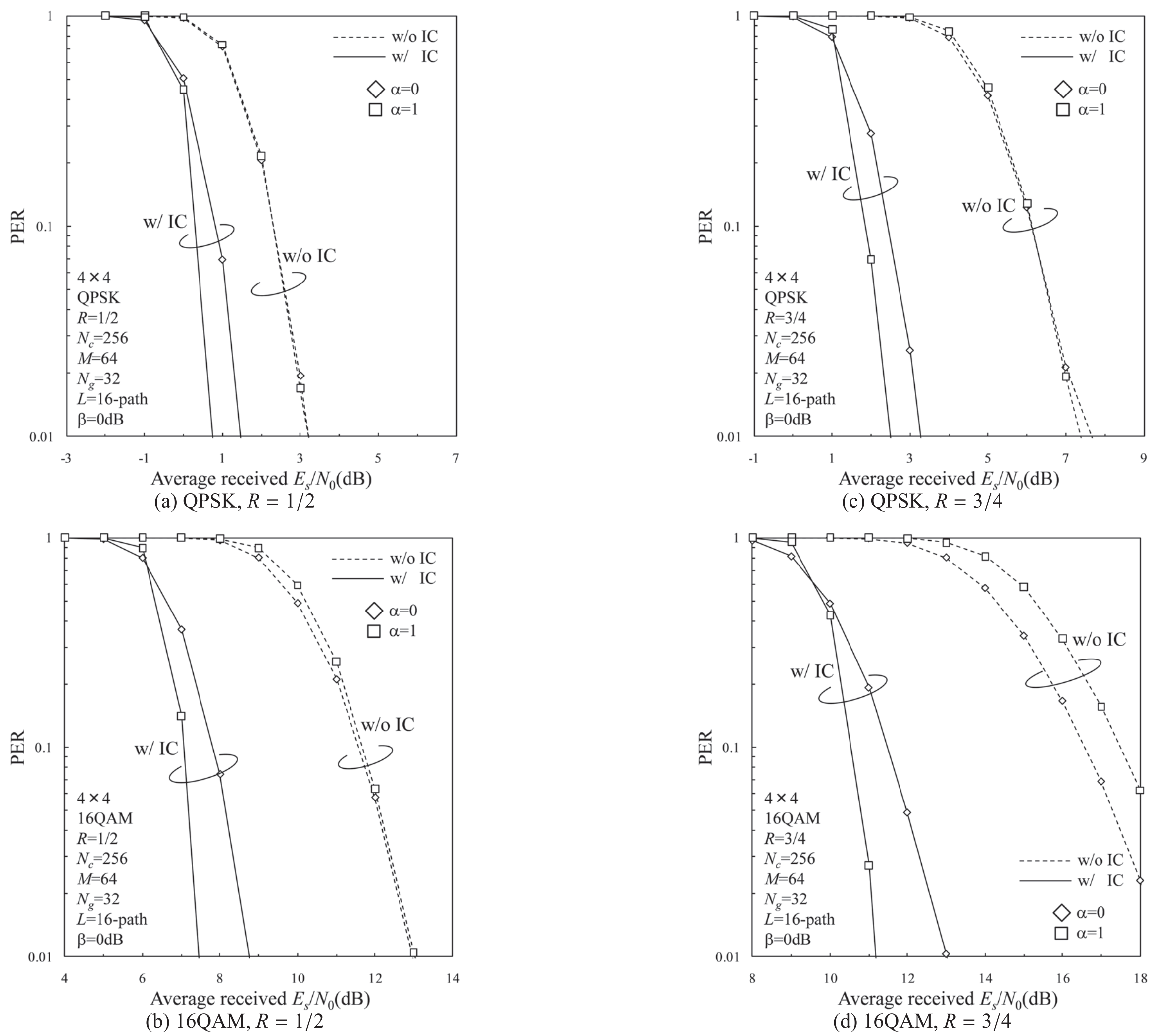

Fig. 4 PER peformance.

number of users can be accommodated. The throughput η(bps/Hz) is defined as

$$\eta = N \times R \times N_t \times \frac{1}{\bar{Q}} \times \frac{1}{1 + N_g/N_c}, \qquad (42)$$

where $\bar{Q}-1$ is the average number of packet retransmissions and N represents the number of bits per symbol.

The throughput performance with IC is plotted as a function of the average received E_s/N_0 in Fig. 5. Two cases of the decay factor β are considered: 0 dB (corresponding to the uniform power delay profile) and 3 dB. For comparison, the throughput performance of OFDMA with IAI cancellation is also plotted assuming $M = 64$ subcarriers, IFFT size $N_c = 256$, and GI size $N_g = 32$. In both SC-FDMA and OFDMA, bit interleaving is used after turbo encoding and puncturing to transform the burst errors into random errors.

At first, the case of β=0 dB (corresponding to the uniform power delay profile) is discussed. It can be seen from Fig. 5 that with MMSED-IC, α=1 provides higher throughput than α=0 over a wide E_s/N_0 region. Larger throughput improvement is seen when higher coding rate ($R = 3/4$) is used. In this case, the coding gain is smaller, but larger frequency diversity gain is obtained. SC-FDMA using $\alpha = 1$ provides higher throughput than OFDMA which has no frequency diversity gain. Next, the case of β=3 dB is discussed. In this case, larger throughput performance improvement over OFDMA is seen than the case of β=0 dB. This is beccause OFDMA obtains smaller coding gain while SC-FDMA obtains relatively larger frequency diversity gain.

The peak E_s/N_0 is an important design parameter which determines the required peak transmit power of terminal transmitter power amplifiers. The throughput performance is plotted as a function of peak E_s/N_0 in Fig. 6 for the case of the decay factor β=0 (corresponding to the uniform power delay profile). The peak E_s/N_0 = is defined as peak E_s/N_0 = average received E_s/N_0+ $\mathrm{PAPR}_{0.1\%}$ [16]. It can be seen from Fig. 6 that the throughput improvement is more pronounced due to the reduced PAPR. The throughput when α=1 shows the highest over a wide E_s/N_0 region.

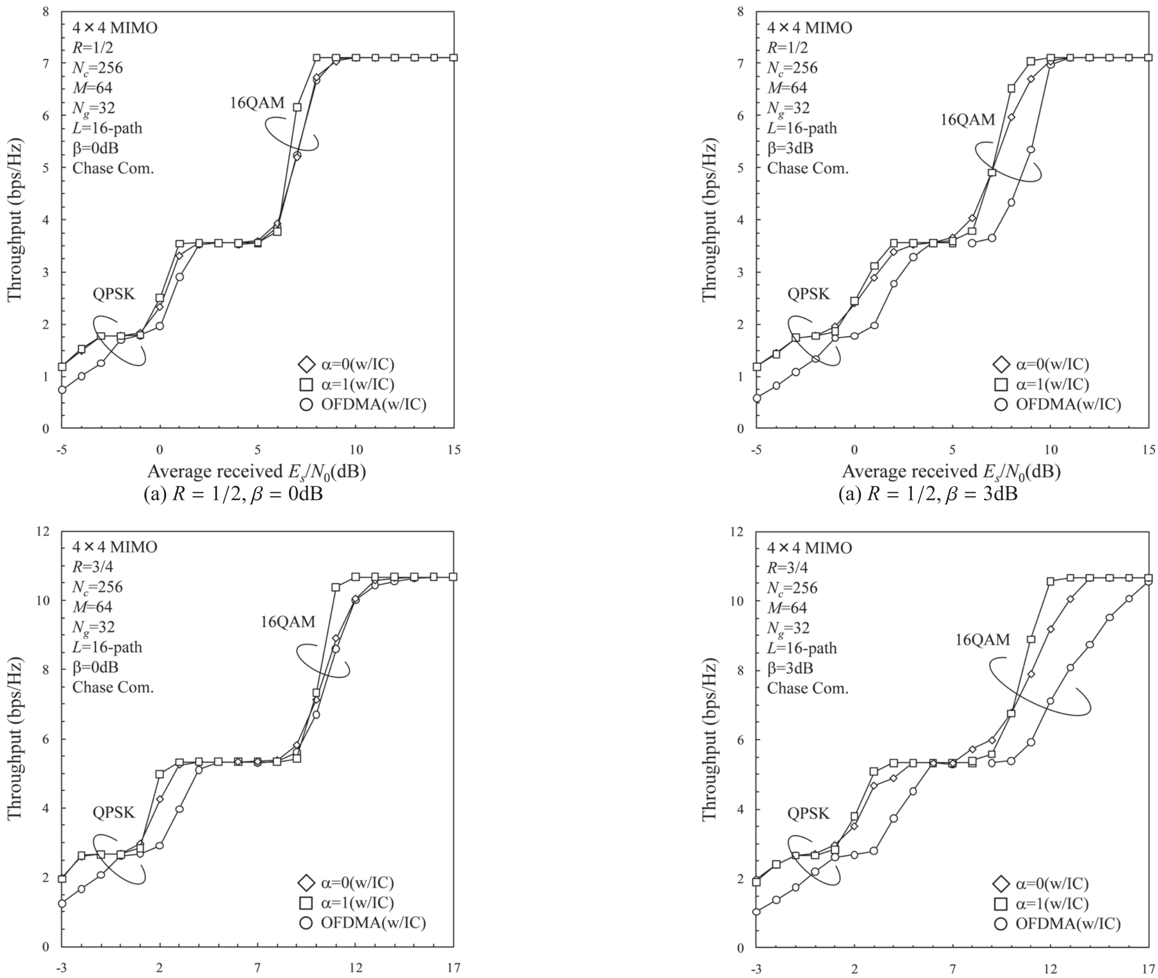

(a) $R = 1/2, \beta = 0$dB (a) $R = 1/2, \beta = 3$dB

(b) $R = 3/4, \beta = 0$dB (b) $R = 3/4, \beta = 3$dB

Fig. 5 Throughput vs. average received E_s/N_0.

5. Conclusion

In this paper, we proposed an iterative MMSE detection and interference cancellation (MMSED-IC) scheme for uplink SC-FDMA MIMO using frequency-domain root Nyquist transmit filtering. By using a transmit filter with roll-off factor $\alpha > 0$, the adjacent users' spectra overlap with the desired signal spectrum and MUI occurs, to deal with the MUI, MUI&IAI&ISI cancellation is performed iteratively at the receiver. The PAPR, PER and throughput performances of the proposed schemes were evaluated by computer simulation. MMSED-IC can improve the PER performance while it can sufficiently suppress MUI&IAI&ISI. We showed that $\alpha = 1$ can achieve better PER performance compared to $\alpha = 0$ while sufficiently suppressing MUI, the additional frequency-diversity gain can be obtained by exploiting the excess bandwidth introduced by the transmit filtering. The throughput performance when $\alpha = 1$ is also higher than when $\alpha = 0$ as well as OFDMA over a wide E_s/N_0 region since larger frequency diversity gain is obtained. The throughput improvement is more pronounced when the throughput performance vs. peak E_s/N_0 is considered.

In a real system, the channel estimation error is present and degrades the HARQ throughput performance when using the proposed iterative MMSED-IC. Therefore, the impact of the channel estimation error on the throughput aachievable by the proposed scheme is practically important and is left as an future study.

References

[1] W.C., Jakes Ir., ed., Microwave mobile communications, Wiley, New York, 1974.
[2] J.G. Proakis, Digital communications, 4th ed., McGraw-Hill, 2001.
[3] R. Prasad, OFDM for wireless communications systems, Artech House, 2004.
[4] S. Hara and R. Prasad, Multicarrier techniques for 4G mobile communications, Artech House, 2003.
[5] J. Armstrong, "New OFDM peak-to-average power reduction scheme," Proc. IEEE 54th Veh. Technol. Conf. (VTC), vol.1, pp.756–760, Oct. 2001.
[6] D. Falconer, S.L. Ariyavisitakul, and A. Benyamin-Seeyarand B.

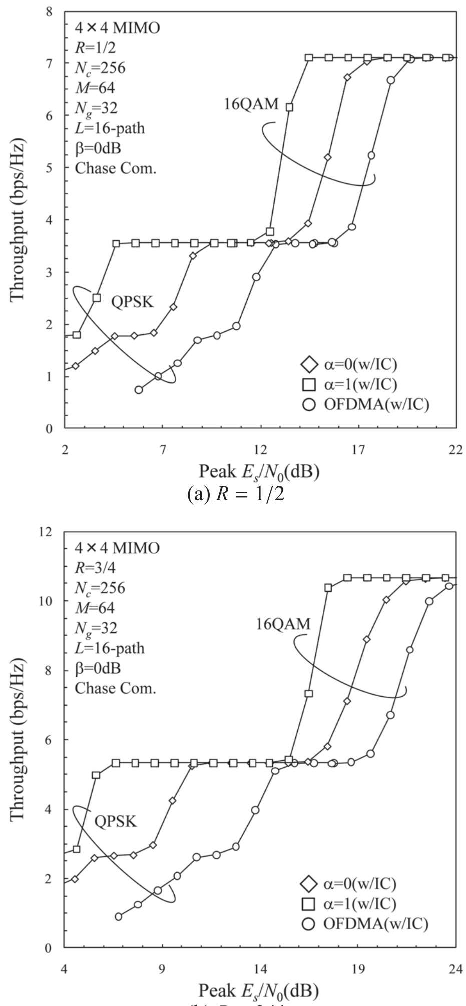

(a) $R = 1/2$

(b) $R = 3/4$

Fig. 6 Throughput vs. peak E_s/N_0.

Edison, "Frequency domain equalization for single-carrier broadband wireless systems," IEEE Commun. Mag., vol.40, no.4, pp.58–66, April 2002.

[7] F. Adachi, D. Garg, S. Takaoka, and K. Takeda, "Broadband CDMA techniques," IEEE Wireless Commun. Mag., vol.12, no.2, pp.8–18, April 2005.

[8] F. Adachi and K. Takeda, "Bit error rate analysis of DS-CDMA with joint frequency-domain equalization and antenna diversity reception," IEICE Trans. Commun., vol.E87-B, no.10, pp.2991–3002, Oct. 2004.

[9] H.G. Myung, J. Lim, and D.J. Goodman, "Single carrier FDMA for uplink wireless transmission," IEEE Vehicular Technology Magazine, vol.3, no.1, pp.30–38, Sept. 2006.

[10] 3GPP, PR-050758, "LS on UTRAN LTE multiple access selection," Nov. 2005.

[11] Y. Akaiwa, Introduction to digital mobile communication, Wiley, New York, 1997.

[12] S. Okuyama, K, Takeda, and F, Adachi, "MMSE frequency-domain equalization using spectrum combining for Nyquist filtered broadband single-carrier transmission," Proc. IEEE 71st Veh. Technol. Conf. (VTC), May 2010.

[13] S. Okuyama, K. Takeda, and F. Adachi, "Frequency-domain iterative MUI cancellation for uplink SC-FDMA using frequency-domain filtering," Proc. IEEE 72nd Veh. Technol. Conf. (VTC), Ottawa, Canada, Sept. 2010.

[14] D. Chase, "Code combining — A maximum-likelihood decoding approach for combining an arbitrary number of noisy packets," IEEE Trans. Commun., vol.CON-33, no.5, pp.385–393, 1985.

[15] K. Takeda, K. Ishihara, and F. Adachi, "Frequency-domain ICI cancellation with MMSE equalization for DS-CDMA downlink," IEICE Trans. Commun., vol.E89-B, no.12, pp.3335–3343, Dec. 2006.

[16] H. Gacanin and F. Adachi, "A comprehensive performance comparison of OFDM/TDM using MMSE-FDE and conventional OFDM," Proc. IEEE 67th Veh. Technol. Conf. (VTC), pp.11–14, May 2008.

Suguru Okuyama received his B.S. degree in Electrical, Information and Physics Engineering in 2009 and M.S. degree in communications engineering, in 2011, respectively, from Tohoku University, Sendai, Japan. His research interests include frequency-domain equalization and multi access interference cancellation for Nyquist filtered single-carrier transmission.

Tetsuya Yamamoto received his B.S. degree in Electrical, Information and Physics Engineering in 2008 and M.S. degree in communications engineering, in 2010, respectively, from Tohoku University, Sendai, Japan. Currently, he is a Japan Society for the Promotion of Science (JSPS) research fellow, studying toward his PhD degree at the Department of Electrical and Communications Engineering, Graduate School of Engineering, Tohoku University. His research interests include frequency-domain equalization and signal detection techniques for mobile communication systems. He was a recipient of the 2008 IEICE RCS (Radio Communication Systems) Active Research Award.

Kazuki Takeda received his B.S., M.S., and Dr. Eng. degrees in communications engineering from Tohoku University, Sendai, Japan, in 2006, 2008, and 2010, respectively. From April 2008 to March 2011, he was a Japan Society for the Promotion of Science (JSPS) research fellow. Since April 2011, he has been with Panasonic Corporation. He was a recipient of the 2009 IEICE RCS (Radio Communication Systems) Active Research Award.

Fumiyuki Adachi received the B.S. and Dr. Eng. degrees in electrical engineering from Tohoku University, Sendai, Japan, in 1973 and 1984, respectively. In April 1973, he joined the Electrical Communications Laboratories of Nippon Telegraph & Telephone Corporation (now NTT) and conducted various types of research related to digital cellular mobile communications. From July 1992 to December 1999, he was with NTT Mobile Communications Network, Inc. (now NTT DoCoMo, Inc.), where he led a research group on wideband/broadband CDMA wireless access for IMT-2000 and beyond. Since January 2000, he has been with Tohoku University, Sendai, Japan, where he is a Professor of Electrical and Communication Engineering at the Graduate School of Engineering. His research interests are in CDMA wireless access techniques, equalization, transmit/receive antenna diversity, MIMO, adaptive transmission, and channel coding, with particular application to broadband wireless communications systems. He is a program leader of the 5-year Global COE Program "Center of Education and Research for Information Electronics Systems" (2007–2011), awarded by the Ministry of Education, Culture, Sports, Science and Technology of Japan. From October 1984 to September 1985, he was a United Kingdom SERC Visiting Research Fellow in the Department of Electrical Engineering and Electronics at Liverpool University. He was a co-recipient of the IEICE Transactions best paper of the year award 1996, 1998, and 2009 and also a recipient of Achievement award 2003. He is an IEEE Fellow and was a co-recipient of the IEEE Vehicular Technology Transactions best paper of the year award 1980 and again 1990 and also a recipient of Avant Garde award 2000. He was a recipient of Thomson Scientific Research Front Award 2004, Ericsson Telecommunications Award 2008, Telecom System Technology Award 2009, and Prime Minister Invention Prize 2010.